

Exploiting Neighbor Effect: Conv-Agnostic GNNs Framework for Graphs with Heterophily

Jie Chen¹, Shouzhen Chen¹, Zengfeng Huang², Junping Zhang¹ and Jian Pu^{3*}

¹Shanghai Key Lab of Intelligent Information Processing and the School of Computer Science, Fudan University

²School of Data Science, Fudan University

³Institute of Science and Technology for Brain-Inspired Intelligence, Fudan University
{chenj19, chensz19, huangzf, jianpu, jpzhang}@fudan.edu.com,

Abstract

Due to the homophily assumption of graph convolution networks, a common consensus is that graph neural networks (GNNs) perform well on homophilic graphs but may fail on the heterophilic graphs with many inter-class edges. In this work, we re-examine the heterophily problem of GNNs and investigate the feature aggregation of inter-class neighbors. To better evaluate whether the neighbor is helpful for the downstream tasks, we present the concept of the neighbor effect of each node and use the von Neumann entropy to measure the randomness/identifiability of the neighbor distribution for each class. Moreover, we propose a Conv-Agnostic GNNs framework (CAGNNs) to enhance the performance of GNNs on heterophily datasets by learning the neighbor effect for each node. Specifically, we first decouple the feature of each node into the discriminative feature for downstream tasks and the aggregation feature for graph convolution. Then, we propose a shared mixer module for all layers to adaptively evaluate the neighbor effect of each node to incorporate the neighbor information. Experiments are performed on nine well-known benchmark datasets for the node classification task. The results indicate that our framework is able to improve the average prediction performance by 9.81%, 25.81%, and 20.61% for GIN, GAT, and GCN, respectively. Extensive ablation studies and robustness analysis further verify the effectiveness, robustness, and interpretability of our framework.

1 Introduction

Recently, emerging graph neural networks (GNNs) have demonstrated remarkable ability for semi-supervised node classification tasks. Most GNNs learn node representation by recursively aggregating neighbor information [Wu *et al.*, 2021; Hamilton *et al.*, 2017]. Under the homophily assumption, i.e., connected nodes tend to be the same class, the

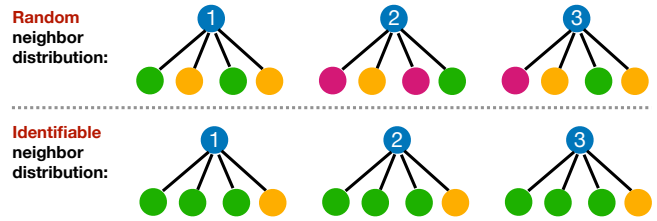


Figure 1: The identifiability of neighbors. Nodes with the same colors share the same class labels. The above neighbor distribution for the blue class is random and the bottom is not random. Although many inter-class edges exist, the identifiable patterns from the non-random distribution of dissimilar neighbors may also help graph convolution classify the center node’s label.

graph convolution, which is often regarded as a Laplacian smoother [Li *et al.*, 2018], smooths each node’s representation by its intra-class neighbors’ representations through the aggregation process to make the classification task profitable. However, the applications of GNNs in heterophilic graphs which connected nodes often have different labels are usually problematic [Nt and Maehara, 2019; Bo *et al.*, 2021; Zhu *et al.*, 2021].

Most existing literature agrees that the massive inter-class edges in heterophilic graphs are harmful for feature aggregation since they may blur the classification boundary and thus decrease the performance for subsequent classification tasks [Pei *et al.*, 2020; Hou *et al.*, 2020; Stretcu *et al.*, 2019]. To evaluate the application performance of GNNs on different graphs and guide the model design, the straightforward homo-ratio based on the proportion of inter-class edges is introduced in [Pei *et al.*, 2020; Zhu *et al.*, 2020]. Although consistent with the homophily assumption, it fails to explain the completely different performance with a similar homo-ratio, as reported in [Zhu *et al.*, 2020]. Therefore, it compels us to re-examine the heterophily problem of GNNs and to answer the following two questions: (1) Is inter-class neighborhood aggregation truly harmful or unnecessary in all cases? (2) How to improve the traditional GNNs’ performance on heterophilic graphs.

As shown in Fig. 1, we first note that the inter-class edges may be beneficial to improve the node classification task if their neighbor distribution is identifiable instead of random.

*To whom correspondence should be addressed.

The critical point is to measure the identifiability of each class. A class with random neighbor distribution is considered to have lower identifiability, whereas an identifiable neighbor distribution is considered to have higher identifiability. An extreme example is the bipartite graph. Although the graph is highly heterophily (each node is connected with the nodes of the opposite class), node features are still distinguishable after a simple mean aggregation operator since their neighbor’s distribution is identifiable [Chien *et al.*, 2021].

Therefore, we present a novel metric to quantify the identifiability of the neighbors of each class and the entire graph. Motivated by this metric, we propose a Conv-Agnostic GNNs Framework (CAGNNs) to improve traditional GNNs’ performance on heterophilic graphs by learning the neighbor effect of each node. We summarize the main contribution as follows.

(1) *We present a novel concept of the neighbor effect and quantify it with Von Neumann entropy.* Instead of considering the inter-class edges perspective, we extract the neighbors’ label distribution matrix at the class level to evaluate the identifiability of neighbors of the entire graph. Specifically, we extend the Von Neumann entropy [Bengtsson and Życzkowski, 2017] as a new metric to quantify the matrix information and measure the identifiability of neighbors of the graph. This metric can explain the performance difference under the same node/edge-homo ratio of some datasets and show that the neighbor effect is vital to understanding and improving the GNN performance. This motivates us to consider the neighbor effect explicitly when performing aggregation for GNNs.

(2) *We propose CAGNNs as a framework to improve traditional GNNs by measuring the neighbor effect for each node.* During the training stage, since the labels may be insufficient to identify the neighbor effect and the neighbor effect for each node may be different when aggregating, we measure the neighbor effect for each node based on the feature and local structures to improve the traditional GNNs. Concretely, we propose a general framework CAGNNs to decouple the features of a node into discriminative features for downstream tasks and the aggregating features from neighbors. Furthermore, we propose a mixer module to adaptively combine these two kinds of features for each node. It learns to determine the neighbor effect and decides whether to absorb or discard the neighbors’ information.

(3) *We conduct extensive experiments on nine well-known benchmark datasets to verify the effectiveness, interpretability, and robustness of CAGNNs.* Our framework can be easily applied to enhance the performance of most GNNs on heterophilic graphs with an additional mixer module.

2 Preliminary

2.1 Problem Setup

Consider an undirected graph $\mathcal{G} = (\mathcal{V}, \mathcal{E})$ with adjacency matrix $\mathbf{A} \in R^{N \times N}$, where \mathcal{V} and \mathcal{E} are the sets of nodes and edges, respectively. For each node $v_i \in \mathcal{V}$, we denote $\mathcal{N}(v_i) = \{j : (i, j) \in \mathcal{E}\}$ as its neighbor set. Each node is given a d -dimensional feature representation \mathbf{x}_i and a c -dimensional one-hot class label \mathbf{y}_i . The feature inputs

Models	Aggregation for each layer $l(1 \leq l \leq L)$
GCN	$h_v^{(l)} = \sigma \left(\sum_{v' \in \mathcal{N}_v \cup \{v\}} \frac{1}{\sqrt{(\mathcal{N}_v +1) \cdot (\mathcal{N}_{v'} +1)}} \cdot W^{(l-1)} \cdot h_{v'}^{(l-1)} \right)$
GIN	$h_v^{(l)} = \text{MLP}^{(l)} \left((1 + \epsilon^{(l)}) \cdot h_v^{(l-1)} + \sum_{v' \in \mathcal{N}(v)} h_{v'}^{(l-1)} \right)$
GAT	$h_{v_i}^{(l)} = \sigma \left(\sum_{v_j \in \mathcal{N}_{v_i} \cup \{v_i\}} a_{i,j}^{(l-1)} \cdot W^{(l-1)} \cdot h_{v_j}^{(l-1)} \right)$

Table 1: The different neighborhood aggregation schemes. Here σ means the ReLU activation, a means attention weights, W means the weight matrix and MLP means multiple layer perceptron.

are then formed by $\mathbf{X} = [\mathbf{x}_1, \dots, \mathbf{x}_N]$, and the labels are $\mathbf{Y} = [\mathbf{y}_1, \dots, \mathbf{y}_N]$. Given the labels $\mathbf{Y}_{\mathcal{L}}$ of a subset of nodes $\mathcal{L} \subset \mathcal{V}$, the task of semi-supervised node classification is to predict the labels $\mathbf{Y}_{\mathcal{U}}$ of the unlabeled nodes $\mathcal{U} = \mathcal{V} \setminus \mathcal{L}$ by exploiting the graph structure \mathcal{E} and the features of nodes \mathbf{X} .

2.2 Graph Neural Networks

From a probabilistic view, most GNNs assume the local Markov property on node features, i.e., for each node v_i , the label y_i only depends on the node self-feature x_i and its neighbor-features $x_j : j \in \mathcal{N}(v_i)$. For the l -th layer of a GNN, we use \mathbf{h}_i^l to represent the embedding of node v_i and \mathbf{h}_i^0 to represent the \mathbf{x}_i or a projection of \mathbf{x}_i for dimension reduction. Then, the general l -th layer Graph Convolution for node i can be formulated as

$$\mathbf{h}_i^{(l)} = f \left(\mathbf{h}_i^{(l-1)}, \left\{ \mathbf{h}_j^{(l-1)} : j \in \mathcal{N}(v_i) \right\} \right), \quad (1)$$

where the graph convolution operator f can be implemented by a weighted sum of each node based on the adjacent matrix \mathbf{A} as in GCN [Kipf and Welling, 2017] and GIN [Xu *et al.*, 2018] or the attention mechanism in GAT [Veličković *et al.*, 2018]. The formulations of three well-known graph convolution layers are summarized in Table 1.

The final output $\mathbf{Z} \in R^{N \times c}$ of the label prediction is evaluated using a *softmax* function to embed the last layer \mathbf{H}^L . The objective function is the cross-entropy of the ground truth labels \mathbf{Y} and the output of the network \mathbf{Z} :

$$\mathcal{O} = - \sum_{i \in \mathcal{L}} \sum_{j=1}^c \mathbf{Y}_{ij} \ln \mathbf{Z}_{ij}. \quad (2)$$

It is worth noting that these GNNs merely use the last layer aggregation feature \mathbf{H}^L for the downstream task which may cause the node classification boundary to be over-smoothed by the corresponding neighbors. Moreover, they ignore the fact that the neighbors’ effect may be different for each individual node.

2.3 Homophily/Heterophily Metrics on Graphs

The homophily ratio h aims to measure the overall homophily level in the graph. By definition, the ratio $h \in [0, 1]$. Graphs with h closer to 1 tend to have more intra-class edges and indicate stronger homophily; on the other hand, graphs with h closer to 0 have more edges connecting different classes and indicate stronger heterophily. The node-level [Pei *et al.*,

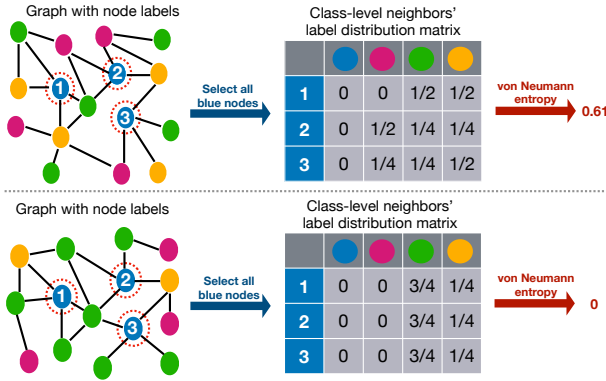


Figure 2: Class-level Von Neumann entropy, which measures the information of neighbors' label distribution matrix. This metric ranges from $[0, 1]$ and can quantify the identifiability of neighbors for a specific class (the lower means the more identifiable).

2020] and edge-level [Zhu *et al.*, 2020] homophily metrics are usually defined by

$$\mathcal{H}_{edge}(\mathcal{G}) = \frac{|\{e_{uv} \mid e_{uv} \in \mathcal{E}, Y_u = Y_v\}|}{|\mathcal{E}|}, \quad (3)$$

$$\mathcal{H}_{node}(\mathcal{G}) = \frac{1}{|\mathcal{V}|} \sum_{v \in \mathcal{V}} \frac{|\{u \mid u \in \mathcal{N}_v, Y_u = Y_v\}|}{d_v}. \quad (4)$$

However, as reported in previous literature [Zhu *et al.*, 2020], these metrics are not significantly relevant to the prediction performance of GCNs. For example, for three well-known heterophily datasets (Chameleon, Squirrel, and Actor), although their homo-ratios are all 0.22, the reported accuracy of node classification for GCN varies, i.e., 60, 37 and 30, respectively [Zhu *et al.*, 2020].

3 A Novel Metric: Von Neumann Entropy to Measure the Neighbor Effect

As noted in Fig. 1, when the distribution of neighbors is random, i.e., every node is randomly connected to others, there is no helpful information we can learn from the aggregation step. However, when the neighbor distribution of each class's nodes forms a certain identifiable distribution, regardless of whether the connected edges are intra-class or inter-class, graph convolution can extract useful information from this non-random neighbor distribution for the downstream tasks. Therefore, we need a new metric to measure the randomness/identifiability of the neighbor distribution.

We define the identifiability of neighbors as the information of the nodes' neighbor distribution. As Fig 2 shows, to measure the identifiability of neighbors, we group the nodes by class and form a neighbor's label distribution matrix $A_{\mathcal{N}}^{c_i} \in R^{m_{c_i} \times C}$ for each class c_i . Then, our task is to evaluate the information of the matrix to quantify the identifiability of neighbors. Inspired by the von Neumann entropy in quantum statistical mechanics [Bengtsson and Życzkowski, 2017], which extends the idea of entropy for positive definite symmetric matrices, we generalize this idea to our task of evaluating neighbors' identifiability.

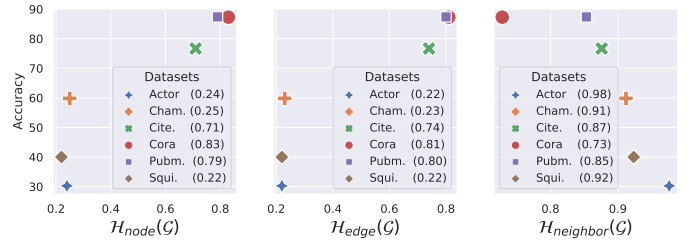


Figure 3: The relation between hom-metric and GCN's performance from [Zhu *et al.*, 2020] on different datasets¹. Our metric is more monotonous with the models' performance and can distinguish the Actor dataset, which has a random neighbor distribution. Other details can be found in Section 5.3.

Specifically, suppose $\sigma_1, \sigma_2, \dots, \sigma_c$ denote singular values of $A_{\mathcal{N}}^{c_i}$, we then normalize them so that $\sum_{i=1}^c \sigma_i = 1$. Then the von Neumann entropy of class c_i is computed by

$$\mathcal{H}_{neighbor}^{c_i} = \frac{-\sum_{i=1}^{n_{c_i}} \sigma_i \log(\sigma_i)}{\log(c)}. \quad (5)$$

Considering the problem of class imbalance, we compute the weighted sum of class-level von Neumann entropy to evaluate the neighbors' identifiability of a graph

$$\mathcal{H}_{neighbor}(\mathcal{G}) = \sum_{c_i=1}^C \frac{n_{c_i}}{N} \mathcal{H}_{neighbor}^{c_i}. \quad (6)$$

Compared with the node/edge-level homophily metrics, our measurement and the GCNs' performance for different datasets are monotonous as shown in Fig. 3. This indicates that the proposed metric can be used to guide the application of GCNs on different datasets. Furthermore, our metric shows that the identifiability of the entire local neighbor is more vital than the proportion of inter-class edges when aggregating. It motivates us to learn the effectiveness of each node's local neighbors when performing graph convolution.

However, to guide the aggregation during the training process, we cannot directly use the entropy measurement and need to evaluate the node-level neighbor effect in another way. The reasons are two-fold: 1) Similar to \mathcal{H}_{edge} and \mathcal{H}_{node} , the computation of the entropy $\mathcal{H}_{neighbor}$ also requires the labels of all the nodes, which are unavailable in the training process. 2) The class-level neighbor distribution identifiability $\mathcal{H}_{neighbor}^c$ is not consistent with the entropy of the node-level label distribution. Namely, the entropy of a node does not represent the identifiability of the neighbor distribution of this class. In the next section, we will elaborate how to adaptively learn the node-level neighbor effect from the downstream supervision signal and the features of a node with its neighbor.

4 Proposed Method and Spectral Analysis

In this section, we first propose the Conv-Agnostic GNNs framework (CAGNNs) to adaptively learn the neighbor effect

¹We ignore the datasets that have fewer than 500 nodes. Their performances are highly sensitive to the data splits.

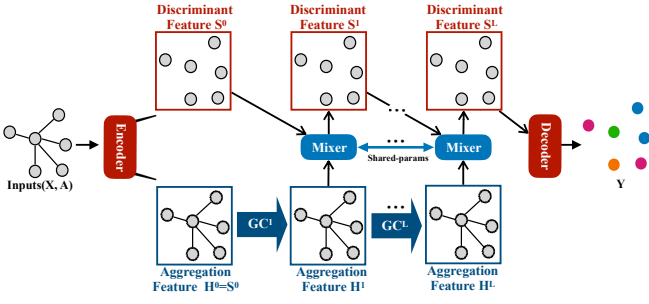


Figure 4: The GC operator indicates any Graph Convolutions. The shared-parameter Mixer function can help each node to determine whether to absorb neighbors’ information by considering the neighbor effect based on the node’s feature.

of each node, followed by a spectral analysis to show the expressive power of the node classification task of the proposed framework.

4.1 Conv-Agnostic GNNs Framework

The proposed CAGNNs aims to empower traditional GNNs to generate suitable representations for each node for both homophilic and heterophilic graphs. The core idea is that we decouple the representation for discrimination and aggregation and learn a mixer module, which can adaptively evaluate the neighbor effect for each node to incorporate the information from its neighborhoods. As shown in Fig. 4, our framework is composed of four major components: Encoder, Graph Convolution, Mixer, and Decoder.

Encoder: We use linear layers as the encoder to transform the node feature \mathbf{X} . Then we feed it into two streams. One is the node’s own feature \mathbf{S}^0 for downstream-task discrimination, and the other is the aggregation feature \mathbf{H}^0 for the graph convolution. The two stream network gives each node the freedom to evaluate the neighbor effect for downstream discrimination tasks in the following aggregation step.

$$\mathbf{H}^0 = \mathbf{S}^0 = \text{Norm}(f_{\text{encoder}}(\mathbf{X})). \quad (7)$$

Graph Convolution: In this part, any standard graph convolution layers (GCN, GAT, GIN) can be applied to aggregate each node’s neighborhood information to update the aggregation representation \mathbf{H} . Moreover, this graph convolution layer can be stacked multiple times to enhance the receptive field of each node by considering the information of more neighbors. The embedding \mathbf{H}^l can also be regarded as the l -hop neighbors’ information, and the following mixer operator is applied to determine the l -hop neighbor effect.

$$\mathbf{H}^{l+1} = \text{Norm}(\text{GraphConvolution}(\mathbf{A}, \mathbf{H}^l)). \quad (8)$$

Mixer: From the view of node v_i at layer l , it need to combine the discrimination feature \mathbf{S}_i^l and l -hop neighbors feature \mathbf{H}_i^l according to the neighbor effect to update the representative embedding for the downstream task. Therefore, the goal of the mixer function is to evaluate the neighbor effect of each node and then selectively incorporate the neighbors’ information. As discussed in Section 3, we do not need to inject the entropy function to evaluate the node-level neighbor effect.

We have already encoded the neighbor information of each node into \mathbf{H}^l by the graph convolution. According to the universal approximation theorem, we hypothesize that the MLP can adaptively learn the node-level neighbor effect based on \mathbf{S}^l and \mathbf{H}^l and the downstream objective \mathcal{O} . For simplicity and better generalization power, we implement the mixer by

$$\alpha^l = \sigma(f_{\text{mix}}(\mathbf{S}^{l-1}, \mathbf{H}^l)), \quad (9)$$

$$\mathbf{S}^l = \text{Norm}((\mathbf{1} - \alpha^l) * \mathbf{S}^{l-1} + \alpha^l * \mathbf{H}^l), \quad (10)$$

where the vector $\alpha^l \in R^{N \times 1}$ denotes the important scores of the neighbors for each node. The function f_{mix} is a linear layer $\in R^{2d \times 1}$, and σ denotes the sigmoid function. Based on the important score α^l , we use the convex combination of discriminant feature \mathbf{S}^{l-1} and neighbor information \mathbf{H}^{l-1} at each layer to adaptively update the discriminant feature \mathbf{S}^l .

Note that the parameters of all the f_{mixer} functions are shared across layers to learn the neighbor effect of each node. Moreover, the mixer function maintains the expressive power of the normal graph convolution, since it can easily degenerate to the normal graph convolution when $\alpha^l = \mathbf{1}$. As shown in the ablation study, our implementation of this mixer function is very effective with minimal parameter cost.

Decoder: With the last layer discriminant \mathbf{S}^L at hand, the task of decoder is to produce the final prediction \mathbf{Z} . For simplicity, we use the linear layer with *softmax* operator as our decoder f_{decoder} .

$$\mathbf{Z} = \text{softmax}(f_{\text{decoder}}(\mathbf{S}^L)). \quad (11)$$

Note that we also apply the L2 norm of each node to maintain numerical stability after the Encoder, Graph Convolution and Mixer module. Compared with the widely used BatchNorm and LayerNorm, the L2 norm of each node is parameter-free and can achieve better performance for our task.

In summary, our CAGNNs contributes three prominent advantages. First, it decouples the discrimination features from the aggregation features in the embedding space for the downstream task so that the graph convolution operator may not directly interact with the node’s discrimination feature and blur the classification boundary. Second, it leverages a learnable mixer function to determine the neighbor’s effect for each node based on these features. It can help each node choose to absorb or discard the neighbors’ information adaptively, thus leading to more discriminative node representations. Third, our framework can easily enhance the performance of most traditional graph convolution layers with only one additional layer.

4.2 Spectral Analysis

Since using a polynomial graph filter can approximate any graph filter [Shuman *et al.*, 2013], the ability to express a polynomial graph filter with arbitrary coefficients is essential to prevent oversmoothing [Chen *et al.*, 2020a] and to learn from heterophilic graphs [Chien *et al.*, 2021].

Theorem 1. *Considering the propagation matrix \mathbf{P} used for the basic Graph Convolution Layer and a graph signal \mathbf{X} , a*

K -layer CAGNNs has the ability to express a K -order polynomial filter $(\sum_l^K \vec{\theta}^l \mathbf{P}^l) \mathbf{X}$ with different arbitrary coefficients θ for each node.

The above theorem indicates the expressive power on node classification of our framework. Intuitively, the important score α allows CAGNNs to simulate the coefficient θ of the polynomial graph filter for each node. Note that with a proper choice of θ , the discriminant feature \mathbf{S}^K of each node can carry information from both the input feature and the high-order neighbor’s information adaptively with the increment of the order K . The detailed proof is presented in Appendix.

5 Experiments

In this section, we report and compare the results for node classification on both real-world heterophily and homophily datasets to investigate the effectiveness, robustness and interpretability of the proposed heterophily GNN framework CAGNNs.

5.1 Experimental Setup

Datasets. We evaluate the performance on nine well-known real-world datasets, including three homophily datasets (Citeseer, Pubmed, and Cora) and six heterophily datasets (Texas, Wisconsin, Actor, Squirrel, Chameleon, and Cornell). For all benchmarks, we use the same feature vectors, graph structures, class labels, and 10 fixed random splits (48%/32%/20% of nodes per class for train/validation/test) provided in literature [Pei *et al.*, 2020; Zhu *et al.*, 2020].

Baselines. We compare our method with the following baselines: (1) traditional standard GNNs: GCN [Kipf and Welling, 2017], GAT [Veličković *et al.*, 2018] and GIN [Xu *et al.*, 2018]; (2) recent state-of-the-art GNNs of specific structure tackling heterophily: Geom-GCN [Pei *et al.*, 2020], MixHop [Abu-El-Haija *et al.*, 2019], H2GCN [Zhu *et al.*, 2020], GPRGNN [Chien *et al.*, 2021], FAGCN [Bo *et al.*, 2021], GCNII [Chen *et al.*, 2020a]; and (3) standard 2-layer MLP.

Hyper-parameters. We adopt the same settings of the default hyper-parameters (2 layers and 64 hidden dimensions) for CAGNNs. For the baselines, we use their best default parameters reported in the original papers. Detailed information of the other hyper-parameters is reported in the Appendix.

5.2 Performance Comparison with SOTA

We report and compare the performance for the standard node classification task in Table 2. We note that the GNNs with specific designs for the heterophily datasets outperform the traditional GNNs (GCN, GIN, GAT) with a large margin for six heterophily datasets. In contrast, taking the neighbor effect of each node into account, our CAGNNs framework helps these GNNs achieve competitive performance to state-of-the-art heterophily GNNs while maintaining the performance on three homophily datasets. The average performance on nine datasets of GIN, GAT, and GCN outperforms all the baselines, and the average performance gains are 9.81%, 25.81%, and 20.61%, respectively. Among them, the proposed CAGNNs with GCN achieves the best average performance over all datasets. It verifies the effectiveness of

decoupling design and consideration of the neighbor effect when performing graph convolution.

5.3 Relation between the Metrics and Performance

Table 2 also shows the different metrics for all datasets. All the metrics range from $[0, 1]$ and a higher score of $\mathcal{H}_{\text{node}}$ and $\mathcal{H}_{\text{edge}}$ denotes higher homophily. However, a higher $\mathcal{H}_{\text{neighbor}}$ means lower identifiability of neighbors’ distribution and a more challenging dataset, i.e., the neighbor distribution provides less useful information for classification. Note that our $\mathcal{H}_{\text{neighbor}}$ can distinguish the dataset Actor (0.98) from others, in which the neighbors’ distribution is nearly random and the best test classification accuracy is very low, i.e., 35.86%. Therefore, neighbor distribution identifiability might provide a new way to understand the heterophily problem in GNNs.

Moreover, we also report the Kendall rank correlation coefficient between the metrics and the performance of CAGNN in Table 3. The $\mathcal{H}_{\text{neighbor}}$ is more correlated with the performance over different datasets. Therefore, the proposed metric can be considered a rough evaluator to measure the difficulty of graphs for the node classification task using GNNs, especially for medium-scale graphs with more than 500 nodes.

For the class-level $\mathcal{H}_{\text{neighbor}}^c$, we show the relation with our CAGNN’s performance under different datasets in Fig. 5. For clarity, we apply the negative $\mathcal{H}_{\text{neighbor}}^c$ for each class to show a positive correlation between the model’s class-wise performance and the class-wise neighbor distribution identifiability. At the class level, we can see that the performance of CAGNN is highly consistent with the neighbor distribution identifiability for most datasets. It also verifies that our framework can adaptively evaluate the neighbor effect for the downstream node classification task.

5.4 Ablation Study

Variants of Mixer. The mixer module is a critical part of our framework to evaluate the neighbor effect and feature fusion. We then compared our results with three variants (Add, Concat and Global) in Table 4. The add mixer is implemented by $\mathbf{S}^l = \text{Norm}(\mathbf{S}^{l-1} + \mathbf{H}^l)$, and the concat mixer is implemented by $\mathbf{S}^l = [\mathbf{S}^{l-1} || \mathbf{H}^l]$. The global mixer is $\mathbf{S}^l = \text{Norm}((1 - \alpha^l)\mathbf{S}^{l-1} + \alpha^l\mathbf{H}^l)$, where the learnable scalar α is shared for all nodes and for each layer. Note that the global mixer is better than the add and concat mixer, which shows that the neighbor effect is diverse under different datasets. Moreover, our mixer is able to adaptively learn the neighbor effect for each node and thus achieves consistently better performance than the global or other variants of mixers.

Variants of Normalization. We also compare the L2 norm for each node with three variants (None, BatchNorm [Ioffe and Szegedy, 2015] and LayerNorm [Ba *et al.*, 2016]) to show its effectiveness. The BatchNorm usually assumes the independent and identical distribution of each sample in deep learning, which may not be reasonable for the heterophilic graph and results in worse performance. On the other hand, LayerNorm is also not beneficial, since the layer norm introduces learning parameters that may be redundant for GNNs. Compared with these variants, our simple yet effective L2 Norm achieves the best average performance.

Table 2: Performance comparison on various real-world heterophily and homophily datasets. Mean test accuracy and standard deviation are reported over 10 random data splits. The best performance is highlighted. “**” denotes the results obtained from [Zhu *et al.*, 2020].

	Texas	Wisconsin	Actor	Squirrel	Chameleon	Cornell	Citeseer	Pubmed	Cora	Average
Nodes	183	251	7,600	5,201	2,277	183	3,327	19,717	2,708	-
Edges	295	466	26,752	198,493	31,421	280	4,676	44,327	5,278	-
Classes	5	5	5	5	5	5	7	3	6	-
\mathcal{H}_{node}	0.06	0.16	0.24	0.22	0.25	0.11	0.71	0.79	0.83	-
\mathcal{H}_{edge}	0.11	0.21	0.22	0.22	0.23	0.30	0.74	0.80	0.81	-
$\mathcal{H}_{neighbor}$	0.45	0.72	0.98	0.92	0.91	0.55	0.87	0.85	0.72	-
GEOM-GCN*	67.57	64.12	31.63	38.14	60.90	60.81	77.99	90.05	85.27	64.05
MixHop*	77.84±7.73	75.88±4.90	32.22±2.34	43.80±1.48	60.50±2.53	73.51±6.34	76.26±1.33	85.31±0.61	87.61±0.85	68.21
H2GCN-1*	84.86±6.77	86.67±4.69	35.86±1.03	36.42±1.89	57.11±1.58	82.16±4.80	77.07±1.64	89.40±0.34	86.92±1.37	70.72
H2GCN-2*	82.16±5.28	85.88±4.22	35.62±1.30	37.90±2.02	59.39±1.98	82.16±6.00	76.88±1.77	89.59±0.33	87.81±1.35	70.87
GPRGNN	82.12±7.72	81.16±3.17	33.29±1.39	43.29±1.66	61.82±2.39	81.08±6.59	75.56±1.62	86.85±0.46	86.98±1.33	70.15
FAGCN	78.11±5.01	81.56±4.64	35.41±1.18	42.43±2.11	56.31±3.22	76.12±7.65	74.86±2.42	85.74±0.36	83.21±2.04	68.18
GCNII	69.72±8.90	75.29±4.64	35.58±1.25	47.21±1.73	60.79±2.35	79.19±6.12	76.82±1.67	89.26±0.48	87.89±1.88	69.07
MLP*	81.89±4.78	85.29±3.61	35.76±0.98	29.68±1.81	46.36±2.52	81.08±6.37	72.41±2.18	86.65±0.35	74.75±2.22	65.99
GIN	71.89±6.64	77.84±4.53	32.15±1.56	35.78±1.34	56.18±1.94	75.94±7.47	75.68±1.89	88.64±0.54	86.49±1.91	66.73
CAGNN _{GIN}	82.51±4.49	84.41±2.98	35.09±1.07	54.07±1.39	67.32±1.95	82.97±5.56	76.64±1.27	89.46±0.48	87.06±1.02	73.28
Gain	↑ 14.77%	↑ 8.44%	↑ 9.14%	↑ 51.12%	↑ 19.83%	↑ 9.26%	↑ 1.21%	↑ 0.93%	↑ 0.66%	↑ 9.81%
GAT*	58.38±4.45	55.29±8.71	26.28±1.73	30.62±2.11	54.69±1.95	58.92±3.32	75.46±1.72	84.68±0.44	82.68±1.80	58.56
CAGNN _{GAT}	83.52±6.17	86.68±3.74	34.95±1.36	55.52±1.45	68.50±1.32	81.35±5.28	75.51±1.54	89.51±0.54	87.48±1.10	73.67
Gain	↑ 43.06%	↑ 56.77%	↑ 32.99%	↑ 81.32%	↑ 25.27%	↑ 38.07%	↑ 0.07%	↑ 5.70%	↑ 5.81%	↑ 25.81%
GCN*	59.46±5.25	59.80±6.99	30.26±0.79	36.89±1.34	59.82±2.58	57.03±4.67	76.68±1.64	87.38±0.66	87.28±1.26	61.62
CAGNN _{GCN}	85.13±5.73	82.55±4.17	35.83±0.73	61.82±1.45	69.16±1.90	81.35±5.47	76.03±1.16	89.74±0.55	87.28±1.01	74.32
Gain	↑ 43.17%	↑ 38.04%	↑ 18.41%	↑ 67.58%	↑ 15.61%	↑ 42.64%	↓ 0.85%	↑ 2.70%	→ 0.00%	↑ 20.61%

Table 3: Kendall correlation between different metrics and the performance of CAGNN_{GCN}.

Datasets	Metrics	\mathcal{H}_{node}	\mathcal{H}_{edge}	$\mathcal{H}_{neighbor}$
>500 nodes	coefficient	0.733	0.828	0.867
	p-value	0.056	0.022	0.017
All datasets	coefficient	0.11	0.25	0.59
	p-value	0.7	0.34	0.02

Table 4: The average performance on all datasets for the ablation study of different types of Mixers and Normalization.

	Variants	CAGNN _{GIN}	CAGNN _{GAT}	CAGNN _{GCN}
Mixer	Add	71.91	70.63	71.41
	Concat	69.50	71.27	72.23
	Global	72.17	72.52	73.43
Norm	None	72.29	73.03	73.01
	BatchNorm	65.11	61.61	64.92
	LayerNorm	72.41	72.19	72.45
Ours	-	73.28	73.67	74.32

5.5 Robustness Analysis

Alleviating oversmooth. It is well known that the traditional graph convolution is sensitive to the number of convolution layers due to the oversmoothing problem [Li *et al.*, 2018]. Our CAGNNs is able to increase the robustness of traditional graph convolution to avoid oversmoothing. As shown in Fig 6(a), when the number of layers increases, the performance of traditional GNNs drops rapidly due to oversmoothing. In contrast, the methods under the proposed framework

are more stable and more consistent on both the Homophily (Citeseer) and Heterophily (Chameleon) datasets. The reason is that our framework has the ability to avoid incorporating the over-smoothing features to maintain the discrimination power for each node.

Alleviating noisy edges. Most GNNs are also sensitive to the noisy edges in graphs [Franceschi *et al.*, 2019; Xu *et al.*, 2019]. To evaluate the robustness of the proposed framework on noisy graphs, we construct graphs with random edge addition according to the literature [Chen *et al.*, 2020b]. Specifically, we randomly add 25%~500% edges in the original graphs. As shown in Fig 6(b), our CAGNNs achieves significantly better prediction for those noisy graphs compared with the basic GNNs. It also demonstrates that our decouple design and the mixer module are able to learn to discard the noisy features from neighbors.

5.6 Visualization and Interpretability

To verify whether CAGNNs can adaptively learn the different neighbor effect of each node, we visualize the coefficients of the neighbor importance score α on different datasets. As shown in Fig 7, most nodes absorb the neighbors’ information in the traditional homophily dataset Cora. However, the neighbor effect of each node is also different. For the traditional heterophily dataset Squirrel, the most neighbor importance scores of the first layer are near 0.8, which shows that nodes still absorb the inter-class neighbors’ information. Moreover, the distribution of the second layer score shows that 1-hop neighbors are more important than the 2-hop neighbors. This indicates that the inter-class edges are not harmful when the neighbors are identifiability. For the Actor dataset in which the neighbor distribution is nearly random (the $\mathcal{H}_{neighbor}$ is 0.98), the neighbor score tends to be

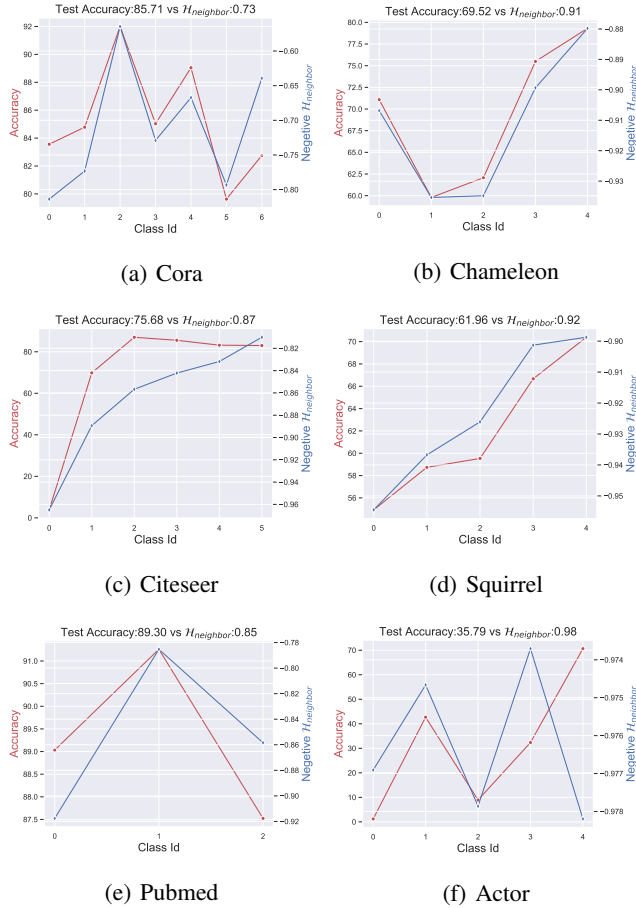


Figure 5: Class-level comparison between our $CAGNN_{GCN}$ performance (red) and the negative class-level $H_{neighbor}^c$ (blue) for Homophily (Cora, Citeseer, and Pubmed) and Heterophily (Chameleon, Squirrel, and Actor).

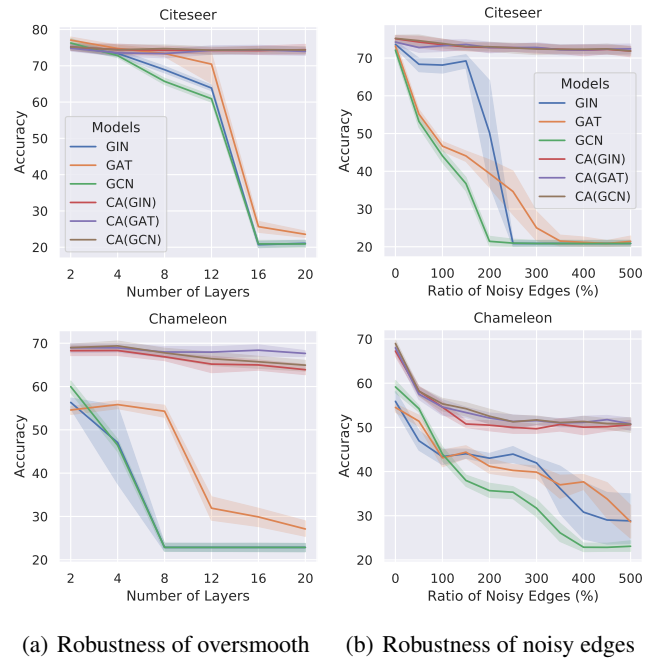
0 so that most nodes consider discarding their neighbors' information. The distribution of coefficient α under different datasets shows that our framework can adaptively choose useful information from a total neighbor perspective.

5.7 Complexity

Finally, we investigate the complexity of the proposed framework. The complexity of computing the neighborhood effect score and mixing for all nodes is $O(|N|d)$ where $|N|$ is the total number of nodes and d is the dimension of hidden nodes. The computational complexity is on par with the neighborhood aggregation operation in GNNs, which is also $O(|N|d)$. We report the average training time of each epoch over all datasets of the standard graph convolution and our method in Appendix.

6 Related Work

Recently, various specific structure GNNs have been proposed to tackle heterophily. Geom-GCN [Pei *et al.*, 2020] utilized structural similarity to capture the smooth structure in the latent space and long-range dependencies. FAGCN [Bo



(a) Robustness of oversmooth (b) Robustness of noisy edges

Figure 6: Performance comparison with traditional GNNs and the variants under the proposed CAGNNs framework in terms of (a) number of layers, and (b) ratio of noisy edges on Homophily (Citeseer) and Heterophily (Chameleon) datasets.

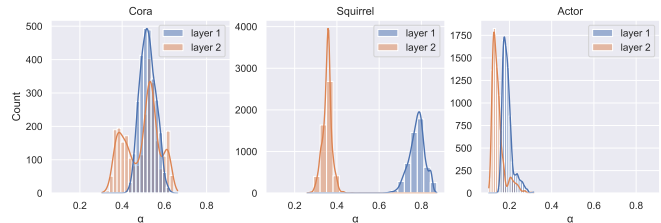


Figure 7: Visualization of nodes' neighbor importance score of the first and second layer on different datasets.

et al., 2021] divided the message from each edge into low-frequency and high-frequency signals. GPRGNN [Chien *et al.*, 2021] modified the convolution to the generalized page rank and learned an arbitrary polynomial graph filter. H2GCN [Bo *et al.*, 2021] proposed three designs with separate ego and neighbors, higher-order neighbors and a combination of intermediate representations to combine the message from neighbors. GCNII [Chen *et al.*, 2020a] proposes a graph convolution with an initial connection and identity mapping to address oversmoothing. Unlike these specific GNN architectures, our framework is compatible with traditional GNNs and can be regarded as a plug-in component to improve their performance on heterophilic graphs.

7 Conclusion

In this paper, we have investigated the neighbor effect on heterophilic graphs and quantified it with von Neumann entropy. The new metric is able to explain the performance

variation of GNNs for different datasets and can be used to guide the application of GNNs. Moreover, we also proposed a general heterophily GNN framework to improve the performance of traditional GNNs. We decouple the features of nodes into discrimination and aggregation, and then use a mixer module to adaptively fuse these features by considering the neighbor effect of each node. Our experiments on nine well-known benchmark datasets demonstrate the effectiveness of our framework to consistently improve existing GNNs on heterophilic graphs.

8 Appendix

8.1 Proof of Theorem 1

For simplicity, we neglect the L2 normalization at each layer because the simplified version also produces comparable performance. We assume the signal vectors \mathbf{S} and \mathbf{H} are non-negative. Then, we have

$$\mathbf{S}^0 = \mathbf{H}^0 \quad (12)$$

$$\mathbf{S}^L = (\mathbf{1} - \mathbf{a}^L) * \mathbf{S}^{L-1} + \mathbf{a}^L * \mathbf{H}^L \quad (13)$$

$$= \sum_{l=0}^L \mathbf{a}^l \prod_{k=l+1}^L (\mathbf{1} - \mathbf{a}^k) * \mathbf{H}^l \quad (14)$$

$$= \sum_{l=0}^L \vartheta^l * \mathbf{H}^l, \quad \text{where } \vartheta^l = \mathbf{a}^l \prod_{k=l+1}^L (\mathbf{1} - \mathbf{a}^k) \quad (15)$$

$$\mathbf{H}^l = \mathbf{P} \mathbf{H}^{l-1} \mathbf{W}^l \quad (16)$$

$$= \mathbf{P}^l \mathbf{H}^0 \prod_j^l \mathbf{W}^j \quad (17)$$

$$= \mathbf{P}^l \mathbf{H}^0 \tilde{\mathbf{W}}^j, \quad \text{where } \tilde{\mathbf{W}}^j = \prod_j^l \mathbf{W}^j \quad (18)$$

$$\mathbf{S}^L = \sum_{l=0}^L \vartheta^l * \mathbf{P}^l \mathbf{H}^0 \tilde{\mathbf{W}}^l \quad (19)$$

However, $\vartheta^l \in [0, 1]$ which limits the expressive power of the polynomial filter. Thanks to the weight matrix $\tilde{\mathbf{W}}^l$, the coefficients of the polynomial can be extended to arbitrary values. Inspired by [Chen *et al.*, 2020a], we consider a weaker version of POGNN by fixing the weight matrix $\tilde{\mathbf{W}}^l$ to be γ^l , where γ^l is a learnable parameter. We have

$$\mathbf{S}^L = \sum_{l=0}^L \vartheta^l * \mathbf{P}^l \mathbf{H}^0 \gamma^l \quad (20)$$

$$= \sum_{l=0}^L \theta^l * \mathbf{P}^l \mathbf{H}^0, \quad \text{where } \theta^l = \vartheta^l \gamma^l \quad (21)$$

The polynomial coefficients θ^l for each layer l can be set to arbitrary values based on the scalable parameter γ^l , so that our framework can help each node to learn arbitrary polynomial graph filters.

8.2 Hyper-parameters Detail

Table 5 summarizes the training configuration of CAGNNs for all datasets. We employ the Adam [Kingma and Ba, 2014] optimizer and select the learning rate

(lr) in $\{0.001, 0.01, 0.05\}$, weight decay (wd) in $\{0, 0.00005, 0.0005\}$ and dropout rate in $\{0, 0.1, 0.5\}$ based on the validation sets.

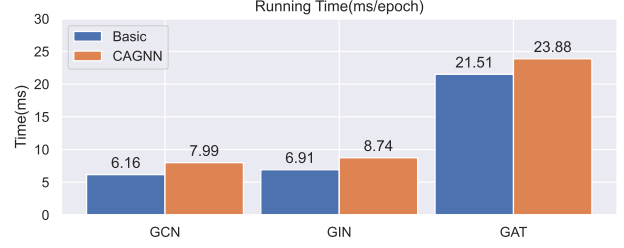


Figure 8: Average running time per epoch (ms)

8.3 Running efficiency

Fig. 8 visualizes the average running time per epoch over all datasets. Our model scales similarly to the basic GNNs with a small computation cost for the mixer module.

Table 5: The other hyper-parameters for Table 2.

Dataset	Method	Hyper-parameters
Texas	CAGNN _{GIN}	lr: 0.01, wd: 0.00005, dropout: 0.5
	CAGNN _{GAT}	lr: 0.01, wd: 0.0005, dropout: 0.5
	CAGNN _{GCN}	lr: 0.05, wd: 0.0005, dropout: 0.5
Wisconsin	CAGNN _{GIN}	lr: 0.01, wd: 0.00005, dropout: 0.5
	CAGNN _{GAT}	lr: 0.05, wd: 0.0005, dropout: 0.5
	CAGNN _{GCN}	lr: 0.01, wd: 0.00005, dropout: 0.5
Actor	CAGNN _{GIN}	lr: 0.05, wd: 0.0005, dropout: 0.5
	CAGNN _{GAT}	lr: 0.05, wd: 0.0005, dropout: 0.5
	CAGNN _{GCN}	lr: 0.05, wd: 0.0005, dropout: 0.5
Squirrel	CAGNN _{GIN}	lr: 0.001, wd: 0.00005, dropout: 0.1
	CAGNN _{GAT}	lr: 0.01, wd: 0.0005, dropout: 0.5
	CAGNN _{GCN}	lr: 0.001, wd: 0, dropout: 0
Chameleon	CAGNN _{GIN}	lr: 0.01, wd: 0.00005, dropout: 0.5
	CAGNN _{GAT}	lr: 0.01, wd: 0.0005, dropout: 0.5
	CAGNN _{GCN}	lr: 0.01, wd: 0.00005, dropout: 0.5
Cornell	CAGNN _{GIN}	lr: 0.01, wd: 0.0005, dropout: 0.5
	CAGNN _{GAT}	lr: 0.01, wd: 0.0005, dropout: 0.5
	CAGNN _{GCN}	lr: 0.05, wd: 0.0005, dropout: 0.5
Citeseer	CAGNN _{GIN}	lr: 0.05, wd: 0.0005, dropout: 0.5
	CAGNN _{GAT}	lr: 0.01, wd: 0.0005, dropout: 0.5
	CAGNN _{GCN}	lr: 0.05, wd: 0.0005, dropout: 0.5
Pubmed	CAGNN _{GIN}	lr: 0.01, wd: 0.00005, dropout: 0.5
	CAGNN _{GAT}	lr: 0.01, wd: 0.0005, dropout: 0.5
	CAGNN _{GCN}	lr: 0.01, wd: 0.00005, dropout: 0.5
Cora	CAGNN _{GIN}	lr: 0.01, wd: 0.0005, dropout: 0.5
	CAGNN _{GAT}	lr: 0.01, wd: 0.0005, dropout: 0.5
	CAGNN _{GCN}	lr: 0.05, wd: 0.0005, dropout: 0.5

References

[Abu-El-Haija *et al.*, 2019] Sami Abu-El-Haija, Bryan Perozzi, Amol Kapoor, Nazanin Alipourfard, Kristina Ler-

- man, Hrayr Harutyunyan, Greg Ver Steeg, and Aram Galstyan. Mixhop: Higher-order graph convolutional architectures via sparsified neighborhood mixing. In *International Conference on Machine Learning*, pages 21–29. PMLR, 2019.
- [Ba *et al.*, 2016] Jimmy Ba, Jamie Ryan Kiros, and Geoffrey E. Hinton. Layer normalization. *preprint arXiv:1607.06450*, 2016.
- [Bengtsson and Życzkowski, 2017] Ingemar Bengtsson and Karol Życzkowski. *Geometry of quantum states: an introduction to quantum entanglement*. Cambridge university press, 2017.
- [Bo *et al.*, 2021] Deyu Bo, Xiao Wang, Chuan Shi, and Huawei Shen. Beyond low-frequency information in graph convolutional networks. In *Proceedings of the AAAI Conference on Artificial Intelligence*, volume 35, pages 3950–3957, 2021.
- [Chen *et al.*, 2020a] Ming Chen, Zhewei Wei, Zengfeng Huang, Bolin Ding, and Yaliang Li. Simple and deep graph convolutional networks. In *International Conference on Machine Learning*, pages 1725–1735. PMLR, 2020.
- [Chen *et al.*, 2020b] Yu Chen, Lingfei Wu, and Mohammed Zaki. Iterative deep graph learning for graph neural networks: Better and robust node embeddings. *Advances in Neural Information Processing Systems*, 33, 2020.
- [Chien *et al.*, 2021] Eli Chien, Jianhao Peng, Pan Li, and Olga Milenkovic. Adaptive universal generalized pagerank graph neural network. In *International Conference on Learning Representations*, 2021.
- [Franceschi *et al.*, 2019] Luca Franceschi, Mathias Niepert, Massimiliano Pontil, and Xiao He. Learning discrete structures for graph neural networks. In *International Conference on Machine Learning*, pages 1972–1982. PMLR, 2019.
- [Hamilton *et al.*, 2017] William L Hamilton, Rex Ying, and Jure Leskovec. Inductive representation learning on large graphs. In *Advances in Neural Information Processing Systems*, pages 1025–1035, 2017.
- [Hou *et al.*, 2020] Yifan Hou, Jian Zhang, James Cheng, Kaili Ma, Richard T. B. Ma, Hongzhi Chen, and Ming-Chang Yang. Measuring and improving the use of graph information in graph neural networks. In *International Conference on Learning Representations*, 2020.
- [Ioffe and Szegedy, 2015] Sergey Ioffe and Christian Szegedy. Batch normalization: Accelerating deep network training by reducing internal covariate shift. *preprint arXiv:1502.03167*, 2015.
- [Kingma and Ba, 2014] Diederik P Kingma and Jimmy Ba. Adam: A method for stochastic optimization. *preprint arXiv:1412.6980*, 2014.
- [Kipf and Welling, 2017] Thomas N. Kipf and Max Welling. Semi-supervised classification with graph convolutional networks. In *International Conference on Learning Representations*, 2017.
- [Li *et al.*, 2018] Qimai Li, Zhichao Han, and Xiao-Ming Wu. Deeper insights into graph convolutional networks for semi-supervised learning. In *Proceedings of the AAAI Conference on Artificial Intelligence*, volume 33, pages 3538–3545, 2018.
- [Nt and Maehara, 2019] Hoang Nt and Takanori Maehara. Revisiting graph neural networks: All we have is low-pass filters. *preprint arXiv:1905.09550*, 2019.
- [Pei *et al.*, 2020] Hongbin Pei, Bingzhe Wei, Kevin Chen-Chuan Chang, Yu Lei, and Bo Yang. Geom-gcn: Geometric graph convolutional networks. In *International Conference on Learning Representations*, 2020.
- [Shuman *et al.*, 2013] David I Shuman, Sunil K Narang, Pascal Frossard, Antonio Ortega, and Pierre Vandergheynst. The emerging field of signal processing on graphs: Extending high-dimensional data analysis to networks and other irregular domains. *IEEE Signal Processing Magazine*, 30(3):83–98, 2013.
- [Stretcu *et al.*, 2019] Otilia Stretcu, Krishnamurthy Viswanathan, Dana Movshovitz-Attias, Emmanouil A Platanios, Sujith Ravi, and Andrew Tomkins. Graph agreement models for semi-supervised learning. In *Advances in Neural Information Processing Systems*, 2019.
- [Veličković *et al.*, 2018] Petar Veličković, Guillem Cucurull, Arantxa Casanova, Adriana Romero, Pietro Liò, and Yoshua Bengio. Graph attention networks. In *International Conference on Learning Representations*, 2018.
- [Wu *et al.*, 2021] Z. Wu, S. Pan, F. Chen, G. Long, C. Zhang, and P. S. Yu. A comprehensive survey on graph neural networks. *IEEE Transactions on Neural Networks and Learning Systems*, 32(1):4–24, 2021.
- [Xu *et al.*, 2018] Keyulu Xu, Weihua Hu, Jure Leskovec, and Stefanie Jegelka. How powerful are graph neural networks? In *International Conference on Learning Representations*, 2018.
- [Xu *et al.*, 2019] Kaidi Xu, Hongge Chen, Sijia Liu, Pin-Yu Chen, Tsui-Wei Weng, Mingyi Hong, and Xue Lin. Topology attack and defense for graph neural networks: An optimization perspective. In *International Joint Conference on Artificial Intelligence*, 2019.
- [Zhu *et al.*, 2020] Jiong Zhu, Yujun Yan, Lingxiao Zhao, Mark Heimann, Leman Akoglu, and Danai Koutra. Beyond homophily in graph neural networks: Current limitations and effective designs. In *Advances in Neural Information Processing Systems*, volume 33, 2020.
- [Zhu *et al.*, 2021] Jiong Zhu, Ryan A Rossi, Anup Rao, Tung Mai, Nedim Lipka, Nesreen K Ahmed, and Danai Koutra. Graph neural networks with heterophily. In *Proceedings of the AAAI Conference on Artificial Intelligence*, volume 35, pages 11168–11176, 2021.